Vibrational Coupling, Isotopic Editing, and β-Sheet Structure in a Membrane-Bound Polypeptide

Cynthia Paul,[†] Jianping Wang,[‡] William C. Wimley,[§] Robin M. Hochstrasser,[*,‡] and Paul H. Axelsen[*,†]

Contribution from the Departments of Pharmacology, Biochemistry and Biophysics, and Medicine, the Johnson Foundation for Molecular Biophysics, and the Department of Chemistry, University of Pennsylvania, Philadelphia, Pennsylvania 19104, and Department of Biochemistry, Tulane University, New Orleans, Louisiana 70112

Received October 3, 2003; E-mail: axe@pharm.med.upenn.edu; hochstra@sas.upenn.edu

Abstract: The N-acetylated hexapeptide WLLLLL (AcWL5) partitions into lipid membranes and is believed to assemble into an antiparallel β-sheet. As a test of this structural assignment, the peptide bonds of residues 2−6 were labeled with ^{13}C and allowed to adsorb onto a supported lipid membrane. Peptides bound to the membrane were examined for evidence of coupling between the labeled vibrational modes in adjacent β-strands with internal reflection infrared spectroscopy. Experimental results indicate that the amide I absorption band in D_2O (i.e., amide I′) attributable to ^{13}C is selectively enhanced when the label is at any one of several positions along the peptide backbone. Simulations employing an excitonic model with through-bond and through-space interactions were performed on AcWL5 models in parallel and antiparallel β-sheet configurations. The simulations yield spectra in good agreement with the experimental results, accounting for the enhancement of both ^{13}C band intensities and band frequencies. They also yield insight into the physical origin and structure selectivity of the distinctive amide I′ band shapes that arise in isotopically edited spectra. It is concluded that the β-sheet formed by membrane-bound AcWL5 is indeed antiparallel, and the enhancement of ^{13}C bands in the infrared spectra of these peptides is caused by both interstrand and intrastrand coupling to ^{12}C modes.

Introduction

β-Sheets are second only to α-helices in prevalence among protein secondary structures, yet model systems in which ordinary small polypeptides form β-sheets in solution are rare. This is in part due to the requirement that sequentially distant residues associate and form a relatively rigid structure without the stabilizing advantage of a hydrophobic core. Model β-sheets that do exist appear to rely on extensive side-chain interactions for their stability.[1,2] Aside from such peptides that probably represent special cases, the formation of β-structure probably requires a molecular template that kinetically seeds or thermo-dynamically stabilizes β-structure among peptides with the potential to form β-structure. For this reason, understanding the role of lipid membranes in promoting β-sheet formation is important and may be essential for understanding the formation of pathological β-structure in protein misfolding diseases such as Alzheimer's disease.

Among the simplest and most thoroughly studied models of β-sheet formation in membranes is the N-acetylated hexapeptide

WLLLLL (AcWL5). AcWL5 is monomeric and random coil in aqueous solution, but it assembles cooperatively to form β-structure upon partitioning into lipid membranes.[3,4] This peptide exhibits a widely split amide I absorption band that is typical of what has come to be regarded as characteristic for antiparallel β-sheet structure, namely a strong component at 1628 cm^{-1} and a weak component at 1679 cm^{-1}. However, there are at least two reasons to question the accuracy of conformational assignments based on this spectral signature. First, aggregated forms of the amyloid β-proteins that accumulate in Alzheimer's disease exhibit the widely split amide I bands characteristic of antiparallel β-structure. Yet, compelling data obtained by various NMR techniques lead to the conclusion that they consist of parallel β-sheets.[5−9] Second, because we lack straightforward model systems for parallel and antiparallel β-sheets, the sensitivity of the split amide I band for antiparallel

† Departments of Pharmacology, Biochemistry and Biophysics, and Medicine, the Johnson Foundation for Molecular Biophysics, University of Pennsylvania.
‡ Department of Chemistry, University of Pennsylvania.
§ Tulane University.

(1) Schenck, H. L.; Gellman, S. H. *J. Am. Chem. Soc.* **1998**, *120*, 4869−4870.
(2) Kortemme, T.; rez-Alvarado, M.; Serrano, L. *Science (Washington, D.C.)* **1998**, *281*, 253−256.

(3) Wimley, W. C.; Hristova, K.; Ladokhin, A. S.; Silvestro, L.; Axelsen, P. H.; White, S. H. *J. Mol. Biol.* **1998**, *277*, 1091−1110.
(4) Bishop, C. R.; Walkenhorst, W. F.; Wimley, W. C. *J. Mol. Biol.* **2001**, *309*, 975−988.
(5) Antzutkin, O. N.; Balbach, J. J.; Leapman, R. D.; Rizzo, N. W.; Reed, J.; Tycko, R. *Proc. Natl. Acad. Sci. U.S.A.* **2000**, *97*, 13045−13050.
(6) Benzinger, T. L. S.; Gregory, D. M.; Burkoth, T. S.; Miller-Auer, H.; Lynn, D. G.; Botto, R. E.; Meredith, S. C. *Biochemistry* **2000**, *39*, 3491−3499.
(7) Burkoth, T. S.; Benzinger, T. L. S.; Urban, V.; Morgan, D. M.; Gregory, D. M.; Thiyagarajan, P.; Botto, R. E.; Meredith, S. C.; Lynn, D. G. *J. Am. Chem. Soc.* **2000**, *122*, 7883−7889.
(8) Antzutkin, O. N.; Leapman, R. D.; Balbach, J. J.; Tycko, R. *Biochemistry* **2002**, *41*, 15436−15450.
(9) Balbach, J. J.; Petkova, A. T.; Oyler, N. A.; Antzutkin, O. N.; Gordon, D. J.; Meredith, S. C.; Tycko, R. *Biophys. J.* **2002**, *83*, 1205−1216.

β-structure and its specificity in the presence of other secondary structure have not been tested. Given that there are reasons to question assignments of antiparallel β-structure secondary structure that are based solely on the presence of a characteristic amide I band shape, it is necessary to confirm this conclusion by alternative means. Nevertheless, it remains advantageous to seek this confirmation using infrared spectroscopy so that confirmation may be obtained from the same samples under the same conditions.

To verify the antiparallel arrangement of β-strands in membrane-bound AcWL5, we synthesized five labeled forms, each containing a single ^{13}C label in its peptide bond. Isotopically editing infrared spectra in this manner has been previously used to facilitate secondary structure assignments in specific portions of a polypeptide.[10-14] The strategy in this case, involving principles first discovered by Rashba[15,16] and used frequently in the study of molecular crystals,[16-18] follows that of Lansbury who showed that transition dipole coupling between isotopically labeled peptide bonds can reveal which bonds on different strands of a β-sheet are in close proximity.[19] Very recently, this approach has been used to explore the relationships between β-strands in a short peptide sequence from the scrapie prion protein.[20] We hypothesized that the spectra emerging from these AcWL5 would exhibit distinctively and predictably different patterns in the cases of parallel and antiparallel β-sheets.

It has been difficult to achieve more than a qualitative interpretation of isotopically edited spectra because the split amide I spectrum of an unlabeled antiparallel β-sheet itself arises from intermode coupling,[21] and the extent of the split appears to depend on the number of polypeptide strands in a sheet.[22] In addition, coupling between peptide bonds containing ^{13}C and ^{12}C appears to result in an enhancement of the signal arising from the label.[14]

To gain a better quantitative understanding of how isotopic editing alters the spectra arising from β-sheets, Brauner et al. studied various ^{13}C-labeled forms of a 14-residue peptide and developed a semiempirical model incorporating both through-space and through-bond interactions to interpret the spectra.[23] Semiquantitative accuracy was achieved in explaining the enhancement of ^{13}C group excitation by coupling to nearby ^{12}C groups through H bonds and valence bonds and the attenuation of ^{12}C group excitation due to the interruption of [12]C−[12]C coupling by interposed ^{13}C groups. Kubelka and Keiderling employed ab initio methods in their examination of spectra from

the same 14-residue peptides, finding that the intensity of the isotopically shifted amide I in ^{13}C-labeled peptides increases with the formation of a multistranded β-structure.[24] Their analysis attributes the intensity increase to in-phase coupled modes among neighboring labeled peptide groups arising from a single predominant ^{13}C mode in the middle of the β-structure. While this approach did not agree with experiment as closely as did that of Brauner et al., it required no adjustable parameters. In studies of other peptides with similar methods, Kubelka and Keiderling found that parallel and various distorted β-sheet structures do not yield highly split amide I bands.[25] The latter may account for the lack of good examples in which proteins exhibit clearly split amide I bands.

It is known that amide-I vibrational modes can be modeled as a subset of individual harmonic oscillators that are coupled to each other but isolated from the rest of the normal modes of a peptide.[10,26,27] Under such conditions, the Frenkel exciton model, a standard model in the treatment of vibrations in molecular crystals,[28] is a reasonable approach to describe their spectra. By assuming that the transition dipole interaction couples the local amide-I′ modes, qualitative agreement has been reached between simulation and experimental FTIR spectra of mid-sized proteins.[26] However, the transition dipole coupling model for the electrostatic, through-space part of the interaction requires an arbitrary choice of origin and is therefore unreliable at distances that are comparable with the size of amide unit undergoing the vibration, in particular between the nearby amide units.

Transition charge coupling and monopole methods have been widely used in electronic spectroscopy[29] to obtain the through-space electrostatic interactions, but they require knowledge of the dynamic charge distributions which rely on computational chemistry. As the separation increases and it no longer matters where the dipole is located in the local mode, the transition charge coupling becomes exactly equal to the dipole−dipole coupling. In our analysis, we have adopted a through-space transition charge−transition charge potential, including charge fluxes for all but the nearest-neighbor amide interactions.[30,31]

We use ab initio density functional theory (DFT) calculations to obtain the total through-bond and through-space contributions to the nearest-neighbor coupling along the polypeptide strands. This approach omits any consideration of dielectric screening (polarizability effects) in gauging through-space couplings. Although there have been numerous attempts to incorporate and develop methods for approximating dielectric screening effects on Coulombic interactions between charges in proteins,[32-38] and

(10) Krimm, S.; Bandekar, J. *Adv. Protein Chem.* **1986**, *38*, 181−364.
(11) Tadesse, L.; Nazarbaghi, R.; Walters, L. *J. Am. Chem. Soc.* **1991**, *113*, 7036−7037.
(12) Decatur, S. M.; Antonic, J. *J. Am. Chem. Soc.* **1999**, *121*, 11914−11915.
(13) Decatur, S. M. *Biopolymers* **2000**, *54*, 180−185.
(14) Silva, R. A. G. D.; Kubelka, J.; Bour, P.; Decatur, S. M.; Keiderling, T. A. *Proc. Natl. Acad. Sci. U.S.A.* **2000**, *97*, 8318−8323.
(15) Rashba, E. I. *Opt. Spektrosk.* **1957**, *2*, 568−577.
(16) Broude, V. L.; Rashba, E. I.; Sheka, E. F. *Spectroscopy of Molecular Excitons*; Springer-Verlag: Berlin, 1985.
(17) Craig, D. P.; Philpott, M. R. *Proc. R. Soc. London, Ser. A* **1966**, *293*, 213−234.
(18) Hochstrasser, R. M.; Whiteman, J. D. *J. Chem. Phys.* **1972**, *56*, 5945−5958.
(19) Halverson, K. J.; Sucholeiki, I.; Ashburn, T. T.; Lansbury, P. T. *J. Am. Chem. Soc.* **1991**, *113*, 6701−6703.
(20) Silva, R. A. G. D.; Barber-Armstrong, W.; Decatur, S. M. *J. Am. Chem. Soc.* **2003**, *125*, 13674−13675.
(21) Krimm, S.; Abe, Y. *Proc. Natl. Acad. Sci. U.S.A.* **1972**, *69*, 2788−2792.
(22) Chirgadze, Y. N.; Nevskaya, N. A. *Biopolymers* **1976**, *15*, 607−625.
(23) Brauner, J. W.; Dugan, C.; Mendelsohn, R. *J. Am. Chem. Soc.* **2000**, *122*, 677−683.

(24) Kubelka, J.; Keiderling, T. A. *J. Am. Chem. Soc.* **2001**, *123*, 6142−6150.
(25) Kubelka, J.; Keiderling, T. A. *J. Am. Chem. Soc.* **2001**, *123*, 12048−12058.
(26) Torii, H.; Tasumi, M. *J. Chem. Phys.* **1992**, *96*, 3379−3387.
(27) Hamm, P.; Lim, M.; Hochstrasser, R. M. *J. Phys. Chem. B* **1998**, *102*, 6123−6138.
(28) Hexter, R. M. *J. Chem. Phys.* **1960**, *33*, 1833−1841.
(29) Smith, P. G.; Gnanakaran, S.; Kaziska, A. J.; Motyka, A. L.; Hong, S. M.; Hochstrasser, R. M.; Topp, M. R. *J. Chem. Phys.* **1994**, *100*, 3384−3393.
(30) Hamm, P.; Lim, M.; DeGrado, W. F.; Hochstrasser, R. M. *Proc. Natl. Acad. Sci. U.S.A.* **1999**, *96*, 2036−2041.
(31) Wang, J.; Hochstrasser, R. M. *Chem. Phys.* **2004**, *297*, 195−219.
(32) Rogers, N. K.; Sternberg, M. J. E. *J. Mol. Biol.* **1984**, *174*, 527−542.
(33) Warshel, A.; Russell, S. T. *Q. Rev. Biophys.* **1984**, *17*, 283−422.
(34) Van Belle, D.; Couplet, I.; Prevost, M.; Wodak, S. J. *J. Mol. Biol.* **1987**, *198*, 721−735.
(35) Taylor, P. L.; Xu, B. C.; Oliveira, F. A.; Doerr, T. P. *Macromolecules* **1992**, *25*, 1694−1698.
(36) Sharp, K.; Jean-Charles, A.; Honig, B. *J. Phys. Chem.* **1992**, *96*, 3822−3828.
(37) Lockhart, D. J.; Kim, P. S. *Science (Washington, D.C.)* **1993**, *260*, 198−202.
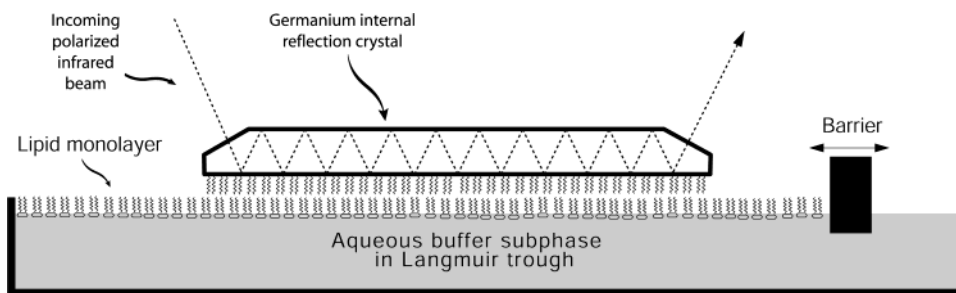
Figure 1. Schematic of the Langmuir trough and internal reflection system used to collect PATIR-FTIR spectra. The germanium crystal is treated with an alkyl-silane to render it hydrophobic. Air-dried samples were studied by applying them directly onto the crystal surface and allowing the solvent to evaporate. Fully hydrated peptide samples were examined by placing the hydrophobic crystal on a phospholipid monolayer at the air−water interface in a Langmuir trough. The log ratio of spectra collected before and after the injection of peptide into the subphase buffer yields an absorption spectrum for membrane-adsorbed peptide.

ensemble dielectric properties are reasonably well understood, there is no rigorous approach for modeling Coulombic interactions at intermediate distances because we lack experimental measurements on specific pairwise interactions. Nevertheless, the approach used in the modeling effort described herein is supported by recent work showing that mode coupling calculated from DFT methods for tri- and tetrapeptides is approximately equal to the transition charge interactions in vacuo for all but nearest neighbors.[31]

Experimental Methods

Unlabeled (UL) and labeled forms of AcWL5 were synthesized by ordinary solid-phase methods as reported previously.[3] A single $^{13}C_1$-labeled leucine residue (Cambridge Stable Isotopes) was placed at amino acid positions 2, 3, 4, 5, or 6 in each of the labeled forms (L2, L3, L4, L5, and L6, respectively).

Polarized attenuated total internal reflection Fourier transform infrared (PATIR-FTIR) spectroscopy was performed using a BioRad FTS-6000 spectrometer equipped with an MCT detector. All spectra (background and sample) are derived from 1024 co-added interferograms with triangular apodization and one level of zero filling. Air-dried samples were examined by mixing 25 μg of peptide with 100 μg of dimyristoylphosphatidylcholine (DMPC, Avanti Polar Lipids) in 30 mM HEPES in D_2O, sonicating for 10 min, and evaporating 5 μL of this mixture onto a horizontal internal reflection crystal (Horizon, Harrick Scientific).

Peptides at the buffer−membrane interface were examined using a Langmuir trough and internal reflection crystal in a manner similar to that described previously (Figure 1).[3] The trough subphase consists of 3 mL of 30 mM HEPES in D_2O, pD=7.4. Lipid monolayer membranes are prepared by applying DMPC to the subphase surface in a few microliters of 90% hexane and 10% ethanol, allowing the solvents to evaporate and compressing the monolayer film to a surface pressure of 20 dynes/cm. The crystal is applied flat onto the subphase surface, and background single-beam spectra were collected. AcWL5 was dissolved in deuterated methanol and introduced through the monolayer and into the magnetically stirred buffer subphase using a microliter syringe and needle to achieve a subphase concentration of approximately 20 μM. Difficulties with sensitivity reported previously have been overcome by design modifications yielding more efficient collection of internally reflected light and by the use of a 30° internal reflection incidence angle which increases the number of internal reflections from 18 to 22 on the sample surface.

Simulation Methods

Molecular all-hydrogen models of AcWL5 were prepared initially as pairs of β-strands in one-dimensional periodic boundaries. One model had two molecules of AcWL5 in a parallel configuration, while the

other model had a pair of AcWL5 molecules in an antiparallel configuration. Both systems were propagated for several hundred picoseconds in vacuo at 300° using CHARMM[39] and then exhaustively energy-minimized. Average parameters were $\phi = -79°$, $\psi = 94°$, $r = 1.9$ Å (H bond length) for the parallel system and $\phi = -114°$, $\psi = 111°$, $r = 2.0$ Å for the antiparallel system.

A series of model sheets with up to 20 AcWL5 molecules for spectral simulation were created by removing the periodic boundaries and juxtaposing a series of β-strand pairs at intervals corresponding to the periodic boundary width. The models were simplified by eliminating all atoms except those in the five peptide units between the six amino acid residues of AcWL5. The amide unit formed at the amino terminus by the acetyl group and the carboxyl terminus were not considered in the simulations even though they participated in interstrand hydrogen bonds (Figure 5).

The polypeptide amide-I′ modes were treated as a set of interacting vibrational harmonic oscillators whose energy levels are separated from the rest of the normal mode vibrations. A Frenkel excitonic model was used to describe the linear-infrared spectra. The Hamiltonian for a particular β-sheet labeled as l, consisting of S polypeptide strands with N amide units in each, can be written as:

$$H^{(l)} = \sum_{n,s}^{N,S} (\epsilon_{ns} + \delta_{ns}^{(l)} - \Delta_{ns}^{(l)})|ns\rangle\langle ns| + \sum_{ns \neq mt} V_{mt,ns}^{(l)}|ns\rangle\langle mt| \quad (1)$$

Here, ϵ_{ns} is the unperturbed vibrational frequency of the relevant transition of the nth amide unit of the sth strand. The $\delta_{ns}^{(l)}$ term allows for site energy fluctuations.[31] The isotopic shift in ϵ_{ns} is given as $\Delta_{ns}^{(l)}$ (zero for $^{12}C={}^{16}O$). The $V_{mt,ns}^{(l)}$ is the interaction terms (coupling energies) between the mtth and nsth amide units. After matrix diagonalization, the eigenstates of $H^{(l)}$ labeled by the index k with their corresponding eigenvalues $E_k^{(l)}$ were obtained for the lth polypeptide.

To simulate the spectra, the zero-order diagonal energy ϵ_{ns} of C=O groups involved in hydrogen bonds was set to ∼1655 cm^{-1}. The zero-order isotopic shift energy $\Delta_{ns}^{(l)}$ needed was found to be ∼39 cm^{-1}, which is within the generally accepted range of ^{13}C isotope shifts (35−45 cm^{-1}).[12,40] For β-sheet configurations with finite size, some of the C=O groups on the first and last strands do not participate in interstrand hydrogen bonding and, depending on the environment, may have vibrational frequencies different from those that are hydrogen-bonded. To simulate the membrane environment, C=O groups on the edge of the sheet and not involved in hydrogen bonds were assigned frequencies 15 cm^{-1} higher than C=O groups involved in hydrogen bonds. No explicit distinction is made between H_2O or D_2O environments in these simulations. However, the effect of H−D exchange is included implicitly in the choice of the diagonal energy and isotope shift, and is designated by a prime (amide I′).

(38) Loffler, G.; Schreiber, H.; Steinhauser, O. *J. Mol. Biol.* **1997**, *270*, 520−534.

(39) Brooks, B. R.; Bruccoleri, R. E.; Olafson, B. D.; States, D. J.; Swaminathan, S.; Karplus, M. *J. Comput. Chem.* **1983**, *4*, 187−217.
(40) Ludlam, C. F. C.; Arkin, I. T.; Liu, X. M.; Rothman, M. S.; Rath, P.; Aimoto, S.; Smith, S. O.; Engelman, D. M.; Rothschild, K. J. *Biophys. J.* **1996**, *70*, 1728−1736.

The square of the length of the net transition dipole of each eigenmode gives the relative contribution of that mode to the linear-IR spectrum, which was obtained as:

$$S(\omega) = \left\langle \sum_k^{NS} \left| \vec{\mu}_{01}^{(k)} \right|^2 \left\{ \frac{\gamma_k/\pi}{\gamma_k^2 + (\omega - \omega_k)^2} \right\} \right\rangle \quad (2)$$
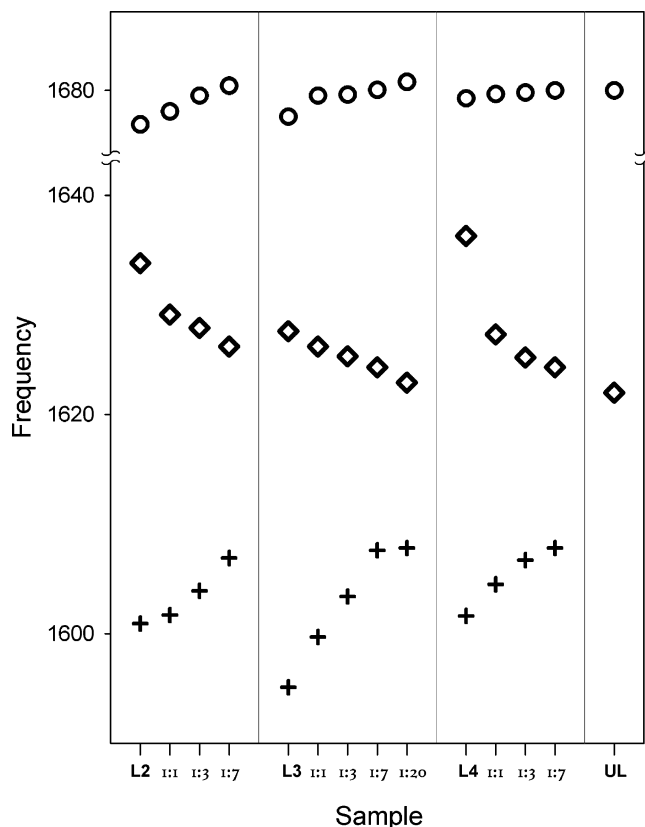
where the angle brackets signify an inhomogeneous average and $\vec{\mu}_{01}^{(k)}$ is the transition dipole for the kth eigenstate of an aggregate. The parameter γ_k models the homogeneous bandwidth for each of the transitions at ω_k. In the simulated IR spectra, when $\gamma_k = 8$ cm^{-1} was used, a satisfactory fit of the experimental IR spectra was obtained with negligible contribution from the frequency fluctuations. This value of γ_k is somewhat larger than the previously determined homogeneous line width (~ 5 cm^{-1}) of amide-I′ modes of short peptides and small proteins in solution phase,[27] suggesting there might be a small inhomogeneous contribution.

The coupling terms $V_{mt,ns}^{(l)}$ were estimated from through-space and through-bond interactions. For all nonnearest neighboring amides along the peptide backbone, a transition charge−transition charge interaction scheme was used.[30,41] The transition charge density was approximated by a distribution of Mulliken charges and charge fluxes. The coupling energy $V_{mt,ns}^{(l)}$ between the mtth and nsth amide units is calculated as follows:

$$V_{mt,ns} = \frac{1}{2} Q_{mt} Q_{ns}$$
$$\left[\sum_{a_{mt},b_{ns}} \frac{\partial^2}{\partial Q_{mt} \partial Q_{ns}} \left(\frac{(q_{a_{mt}}^0 + \delta q_{a_{mt}}^0 Q_{mt})(q_{b_{ns}}^0 + \delta q_{b_{ns}}^0 Q_{ns})}{r_{a_{mt},b_{ns}}} \right) \right]_{Q_{mt} = Q_{ns} = 0} \quad (3)$$

Here, subscripts a, b, ... label all the atoms undergoing nuclear displacements in the coupled amide-I′ units. The equilibrium atomic coordinates were obtained from the β-sheet model prepared using molecular mechanics and described above. The charge at the atom a_{mt} is $q_{a_{mt}}^0$ at equilibrium, Q_{mt} is the dimensionless normal coordinates for the mtth amide, $\delta q_{a_{mt}}^0$ is the charge flux, $[\delta q/\delta Q]_0$, at atom a_{mt}, and $r_{a_{mt},b_{ns}}$ is the distance between the indicated atoms. A set of transition charges was obtained from ab initio DFT calculation on a monopeptide model compound *N*-methyl-acetamide using Gaussian-98[42] at the B3LYP/6-31+G* level.[30,41] The calculated charge distribution had a transition dipole of 3.8 D/(Å amu$^{1/2}$), directed at 20° to the C=O bond in agreement with previous empirically chosen values.[43] Equation 3 becomes the transition dipole−dipole interaction at large intermode distances.

The total coupling strength, including both the through-bond and through-space contributions for two amide-I′ modes in adjacent peptide units, was evaluated via an ab initio DFT calculation based on the dipeptide model *Ac-Gly-NMe* using Gaussian-98[42] at the B3LYP/6-31+G** level. It is known that the coupling energy between the nearest-neighbor amides is torsional angle dependent, and therefore, we evaluated this

(41) Hamm, P.; Hochstrasser, R. M. Structure and dynamics of proteins and peptides: femtosecond two-dimensional infrared spectroscopy. In *Ultrafast Infrared and Raman Spectroscopy*; Fayer, M. D., Ed.; Marcel Dekker: New York, 2001; pp 273−347.
(42) Frisch, M. J.; Trucks, G. W.; Schlegel, H. B.; Scuseria, G. E.; Robb, M. A.; Cheeseman, J. R.; Zakrzewski, V. G.; Montgomery, J. A., Jr.; Stratmann, R. E.; Burant, J. C.; Dapprich, S.; Millam, J. M.; Daniels, A. D.; Kudin, K. N.; Strain, M. C.; Farkas, O.; Tomasi, J.; Barone, V.; Cossi, M.; Cammi, R.; Mennucci, B.; Pomelli, C.; Adamo, C.; Clifford, S.; Ochterski, J.; Petersson, G. A.; Ayala, P. Y.; Cui, Q.; Morokuma, K.; Malick, D. K.; Rabuck, A. D.; Raghavachari, K.; Foresman, J. B.; Cioslowski, J.; Ortiz, J. V.; Stefanov, B. B.; Liu, G.; Liashenko, A.; Piskorz, P.; Komaromi, I.; Gomperts, R.; Martin, R. L.; Fox, D. J.; Keith, T.; Al-Laham, M. A.; Peng, C. Y.; Nanayakkara, A.; Gonzalez, C.; Challacombe, M.; Gill, P. M. W.; Johnson, B. G.; Chen, W.; Wong, M. W.; Andres, J. L.; Head-Gordon, M.; Replogle, E. S.; Pople, J. A. *Gaussian 98*, revision A.9; Gaussian, Inc.: Pittsburgh, PA, 1998.
(43) Cheam, T. C.; Krimm, S. *Chem. Phys. Lett.* **1984**, *107*, 613−616.

Figure 2. Behavior of amide I absorption components in ^{13}C-labeled AcWL5 upon dilution with unlabeled peptide. The spectra generally resemble the experimental spectra in Figure 3, but differ slightly because the samples are air-dried rather than fully hydrated. The position of the absorption maxima for the ^{13}C (+), ^{12}C ($\diamond$), and high-frequency ($\circ$) bands are plotted versus label position and dilution. Data for L2, L3, L4, and UL represent pure peptides. Ratios 1:1, 1:3, 1:7, and 1:20 indicate that one part labeled peptide was mixed with 1, 3, 7, or 20 parts UL peptide prior to mixing with lipid.
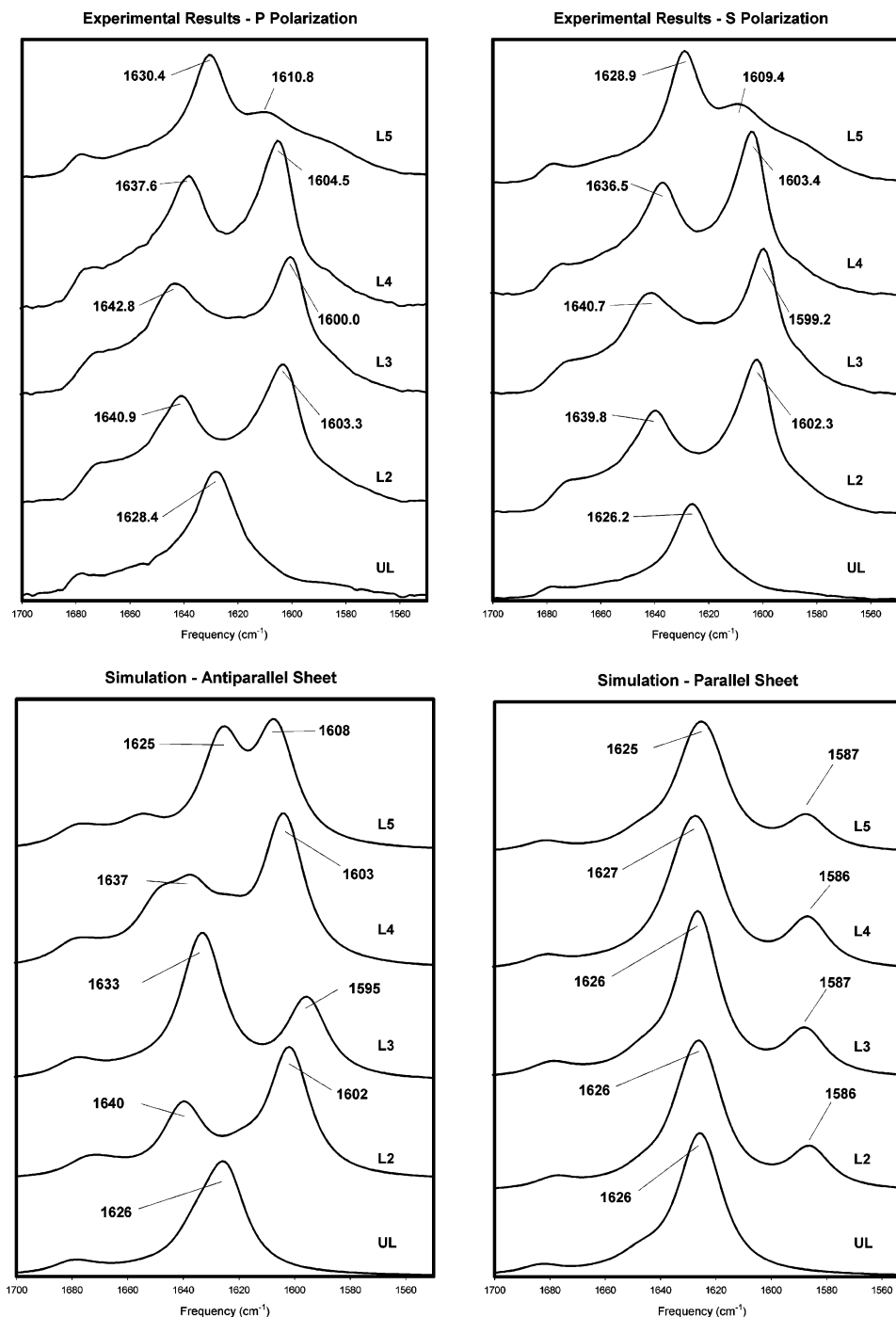
coupling for the average torsional angle of the β-sheet conformation. A partial optimization was performed with a fixed specific set of dihedral angles in the range of configurations of antiparallel β-sheets.

We confirmed that the amide-I′ frequencies are adequately reproduced by a Hamiltonian matrix diagonalization procedure based on equal diagonal elements and a set of transferable coupling constants. A normal-mode analysis was carried out on the optimized geometries, and coupling energies were obtained. When the dipeptide was chosen with dihedral angles of $-110°$ and $+115°$, the symmetric (high-frequency) and antisymmetric (low-frequency) amide-I′ normal modes were split by 6.6 cm^{-1}. Linear combinations with approximately equal weight of these two modes generated two *localized* amide-I′ modes. Therefore, the amide-I′ modes of *Ac-Gly-NMe* can be modeled reasonably by two degenerate local modes coupled by $\sim +3.3$ cm^{-1}. This result suggests that we employ $V_{ns,ns+1} \approx +3.3$ cm^{-1} as the average coupling between the intrastrand nearest neighbors of the antiparallel β-sheets. This idea has been checked with DFT calculations of tri- and tetrapeptides.[31] For a dipeptide in the configuration of parallel β-sheets ($-79°$, $+94°$), we found the coupling energy between the intrastrand nearest neighbors to be $V_{ns,ns+1} \approx -3.5$ cm^{-1}, which is quite different from the result for antiparallel β-sheets because of the dihedral angle dependence of through-bond effects.

Results

Initial experiments with air-dried peptide−lipid mixture samples yielded spectra from UL similar to those previously reported for membrane-bound samples,[3] with strong absorption at 1622 cm^{-1} and weaker absorption at 1680 cm^{-1} (Figure 2). Spectra

Figure 3. Amide I spectra for UL, L2, L3, L4, and L5 (arbitrary vertical scales). Above: PATIR-FTIR spectra for parallel (left) and perpendicular (right) polarized light. Labeled frequencies are the local absorption maxima. Below: simulated spectra for antiparallel (left) and parallel (right) β-sheets.

from air-dried L2, L3, and L4 peptide−lipid mixtures exhibited a primary absorption band component between 1595 and 1601 cm^{-1}, a secondary component between 1627 and 1636 cm^{-1}, and a weak component centered between 1673 and 1679 cm^{-1}. Both the primary and secondary components of L3 had significantly lower frequencies than the corresponding components in L2 and L4. Upon mixing with increasing amounts of unlabeled peptide, the primary amide I′ absorption component of L2, L3, and L4 shifted to higher frequencies and diminished in intensity relative to the secondary component, while the secondary amide I′ component shifted to lower frequencies, approaching that of the UL peptide. L5 exhibited a minor component at 1609 cm^{-1} that disappeared upon mixing with UL, while the

Table 1. Principal Amide I Absorption Band Frequencies

peptide	simulation parallel strands		simulation antiparallel strands		experimental parallel polarization		experimental perpendicular polarization	
UL	1626		1626		1628.4		1626.2	
L2	1626	1586	1640	1602	1640.9	1603.3	1639.8	1602.3
L3	1626	1587	1633	1595	1642.8	1600.0	1640.7	1599.2
L4	1627	1586	1637	1603	1637.6	1604.5	1636.5	1603.4
L5	1625	1587	1625	1608	1630.4	1610.8	1628.9	1609.4

spectrum of L6 was indistinguishable from that of UL. Control experiments with UL but no lipid exhibited a single featureless amide I′ absorption band at 1643 cm^{-1} (not shown). Overall,
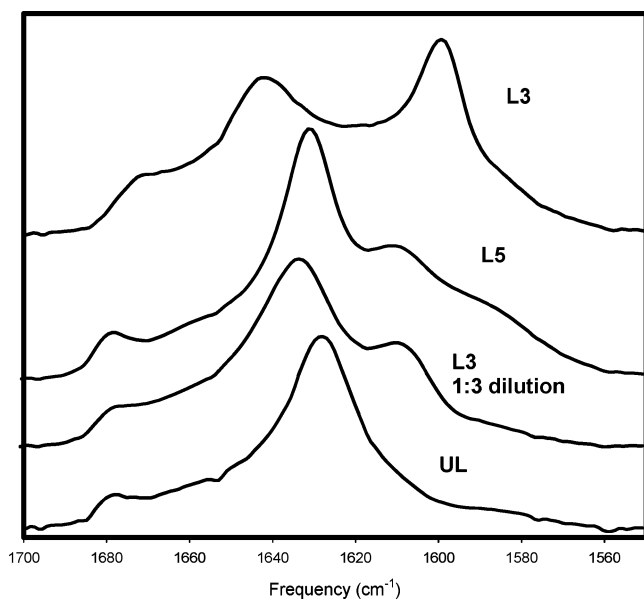
Figure 4. PATIR-FTIR spectra comparing L5 with L3, UL, and a 1:3 mixture of L3 and UL (arbitrary vertical scales).

the data from air-dried samples demonstrate that the frequencies and relative intensities of both the ^{12}C and ^{13}C peaks depend on the proximity of the ^{13}C labels to each other.

Spectra from fully hydrated peptides at the buffer−membrane interface are much more challenging to obtain, but offer the advantage of more biologically relevant conditions, and they yield information about peptide orientation in the membrane. In general, we find that monolayers yield results that are qualitatively similar to air-dried peptide−lipid mixtures, but band frequencies are red-shifted to varying degrees (Table 1). The primary absorption component maximum for L2, L3, and L4 was between 1599 and 1605 cm^{-1}, while the secondary component maximum was between 1636 and 1643 cm^{-1} (Figure 3). L5 again exhibits a minor component at 1609−1610 cm^{-1}, while L6 is indistinguishable from UL. When L3 is diluted 1:3 with unlabeled peptide, a spectrum closely resembling the L5 spectrum is obtained (Figure 4).

There are three significant patterns in these data. First, the maximum amplitudes in spectra arising from air-dried specimens are 2−5 cm^{-1} red-shifted relative to fully hydrated peptides at the buffer−membrane interface. Second, the maximum arising from L3 is red-shifted by 3−4 cm^{-1} relative to that of L2 and L4. Third, the maxima arising from *s*-polarized spectra are red-shifted by 0.8−1.1 cm^{-1} relative to those of *p*-polarized spectra. This third pattern is subtle, but it suggests that the most red-shifted absorption modes in the samples are also the most horizontally oriented. The dichroic ratio for the principal amide I′ components of L2, L3, and L4 is 1.4, corresponding to an order parameter of −0.26 on this instrument for which the internal reflection incidence angle was 30°. The ratio of 1.3 previously reported corresponds to the same order parameter because it was obtained on an instrument with an internal reflection incidence angle of 45°.[3]

The simulated spectra for the antiparallel β-sheets reproduce several key features of the experimental data (Figure 3). First, the frequencies of local amplitude maxima for each of the principal components are all within 3 cm^{-1} of the experimental values (table). Second, they reproduce the pattern noted above

in which L3 is red-shifted to a greater degree than L2 and L4. Third, the relative intensities of the two main components in L2 and L4 are close to the experimental spectra. The antiparallel simulation does not correctly predict the relative amplitudes of the two main components of L3, and it predicts an enhancement of the ^{13}C peak in L5 that is not seen experimentally.

While the agreement between the experimental frequencies and isotope intensity enhancement and the antiparallel simulation varies from excellent for L2 and L4 to fair for L3, there is little agreement between experimental spectra and the parallel simulations. Indeed, the parallel simulations yield almost indistinguishable spectra for L2, L3, L4, and L5, as one might expect intuitively from a series of peptides in which spatial relationships among [12]C=O and [13]C=O groups are similar irrespective of label position. Moreover, none of the parallel simulations predict the large enhancement of ^{13}C modes that is among the most conspicuous features of the experimental spectra.

Discussion

These results indicate that AcWL5 assembles as an antiparallel β-sheet in lipid membranes. The antiparallel simulations accurately predict the pattern of band positions and intensities observed in the experimental spectra, whereas the parallel simulation predicts spectra with little resemblance to the experimental spectra. These results, in tandem with previously reported studies,[3] weigh strongly in favor of an antiparallel β-sheet for AcWL5 in lipid membranes.

Apart from the simulations, it is difficult to determine whether AcWL5 adopts parallel or antiparallel β-sheet structure solely based on the isotopically edited experimental spectra. On one hand, the ^{13}C peak of L3 is more red-shifted than that of L2 or L4. This might be interpreted to mean that the labels in adjacent L3 peptides are in closer proximity than those in L2 or L4, and this will be the case in antiparallel, but not parallel, β-sheets (Figure 5). On the other hand, the similarities among spectra from L2, L3, and L4 are more striking than their differences. All three peptides give rise to components with similar relative amplitudes located within 5 cm^{-1} of each other, and this might be expected to arise in a parallel β-sheet because labels should be equidistant in L2, L3, and L4. Thus, simulations are very useful in interpreting the experimental spectra, and the anomalous intensity enhancement of ^{13}C modes seen in the antiparallel, but not the parallel, β-structures is key to this interpretation.

The simulations yield insight into the physical basis for the selective enhancement of ^{13}C band intensities.[44] As illustrated in Figure 6, the unperturbed exciton band structures of the antiparallel and parallel β-sheets are similar except that the density of states maximizes on the lower energy side of the band in the parallel sheet and on the higher energy side in the antiparallel sheet. In both cases, the strongly allowed transition at or near the bottom of the band is a delocalized mode in which adjacent amide-I′ modes are oscillating in-phase interstrand but out-of-phase intrastrand. This picture was verified by inspection of the wave function coefficients. The interaction of the ^{13}C-substituted site with the unsubstituted sites causes levels to split off the bottom of the exciton band.[17] The relative intensity of the two low-frequency-allowed modes that result is very

(44) Moore, W. H.; Krimm, S. *Proc. Natl. Acad. Sci. U.S.A.* **1975**, *72*, 4933−4935.
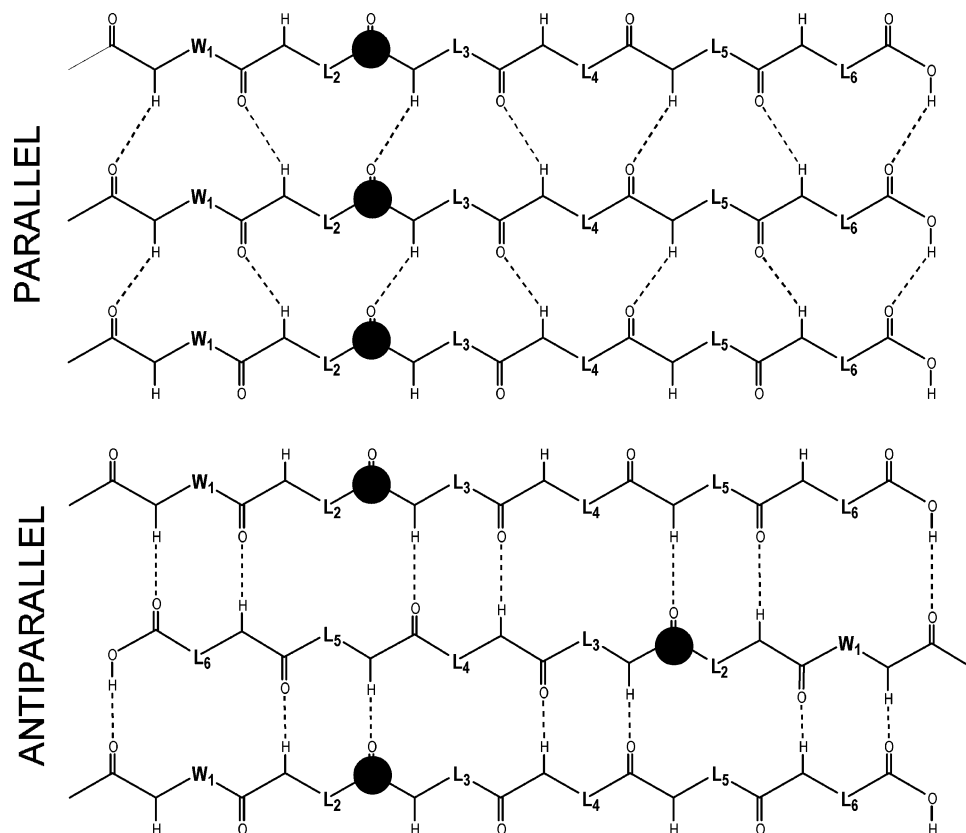
Figure 5. Labeling pattern for parallel and antiparallel *β*-sheet forms of AcWL5. Large black dots mark the position of the ^{13}C label if these structures are adopted by L2. In the parallel case, labels in L2 are closely apposed in the same way that labels would be for peptides labeled at other positions. In the antiparallel case, the labels of L2 are further apart, similar to the way that labels would be for L4. The labels of L3 would be closely apposed in both the parallel and antiparallel sheets.
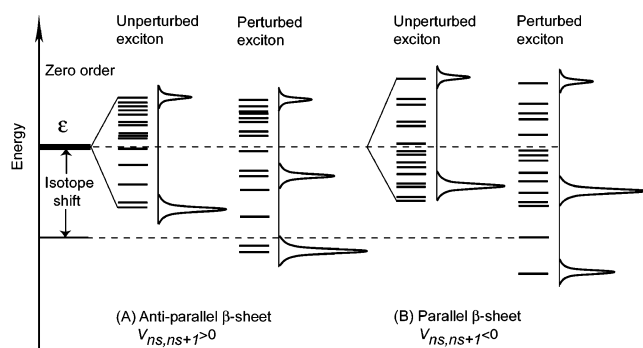
Figure 6. Exciton band structures and IR spectra of the antiparallel and parallel *β*-sheets in zero order, unperturbed and perturbed by ^{13}C-substitution. The nearest-neighbor coupling along the strand is $V_{ns,ns+1}$.

sensitive to the sign of the intrastrand nearest-neighbor coupling $V_{ns,ns+1}$, while the separation between them is sensitive to the zero-order isotope shift (see Figure 6). In the case of the antiparallel *β*-sheet, $V_{ns,ns+1} > 0$ and the lower frequency mode has higher intensity since the ns^{th} and $(ns + 1)$th amide-I′ motions along the strand are out-of-phase. In the case of the parallel *β*-sheet, $V_{ns,ns+1} < 0$, the lowest frequency mode has the lowest intensity. Therefore, the most important coupling was identified as $V_{ns,ns+1}$. There is a simple explanation for these coupling inequalities and the enhancement, based on the interactions of pairs. Consider pairs of ^{12}C=^{16}O and ^{13}C=^{16}O vibrators, with the latter at lower frequency. A positive coupling intensifies the lower state of the interacting pair if the carbonyl groups are antiparallel as occurs along a strand. The negative interaction between parallel carbonyls, as occurs between

strands, intensifies the lower states of interacting pairs. The reasoning is based on the eigenvectors of two-level systems, which predict a fractional difference in intensity of the ^{13}C=^{16}O and ^{12}C=^{16}O transitions that is proportional to $\pm\cos\theta$, where θ is the angle between the C=O groups of the components of the pair and the $\pm$ chooses the sign of the coupling constant.

To have intensification of the ^{13}C modes, they must couple with the ^{12}C modes in an optimal manner. For example, a ^{13}C-substituted mode on one chain should have a ^{12}C mode as its nearest neighbor on the adjacent chain. This is the case for all antiparallel sheets except L3, but it is never the case for the parallel sheet. The coupling patterns for the two *β*-sheet conformations, therefore, have different topologies. The coupling between hydrogen-bonded pairs for both *β*-sheet conformations was found to be ~-11.0 cm^{-1} ($V_{ns,(N-n+1)(s+1)}$ in the antiparallel and $V_{ns,n(s+1)}$ in the parallel), by using transition charge–transition charge interactions. The next nearest-neighbor intrastrand coupling energy ($V_{ns,ns+2}$) was found to be between $+2.0$ and $+3.0$ cm^{-1} for both *β*-sheet conformations, confirming that the intrastand in-phase coupling is a minor contribution to the ^{13}C-peak enhancement in the antiparallel *β*-sheet. The significant difference in $V_{ns,ns+1}$ for the two *β*-sheets causes the band to spread more toward the lower energy side with respect to its zero-order level for the antiparallel configuration, so as to increase the chance of strong mixing between the dipole-allowed bulk excitonic state and the isotope state. In the case of the parallel *β*-sheet with $V_{ns,ns+1} < 0$, the band spreads more toward higher energies. In addition, our calculation shows that the

strongly allowed transition in the parallel β-sheet does not occur at the bottom of the exciton band, which limits the IR transition intensity transfer from the bulk to the trap.

The ^{13}C-peak intensity enhancement is dependent on the number of strands per sheet, S. When S is 1 or 2, the interstrand coupling is not effective in causing a significant enhancement. As S increases, the enhancement becomes larger and eventually saturates at $S \geq 9$. The fit of simulation to experimental data suggests that S is in the range of $\sim$3 to 4 in the antiparallel β-sheets. The main uncertainty in making this assessment is the magnitude of the intrastrand nearest-neighbor coupling because it is very sensitive to the dihedral angles that vary within the structure. We find from ab initio calculations that by varying the dihedral angles by $\pm 10°$, a change of ± 1 cm^{-1} can be introduced into $V_{ns,ns+1}$. When $V_{ns,ns+1}$ is chosen as $+3.3$ cm^{-1} we find that $S = 3$, but $S = 4$ gives the best fit when $V_{ns,ns+1} = 2.3$ cm^{-1}. There may be some mismatch between adjacent strands in the samples used in the experiment; this could be the explanation as to why the ^{13}C enhancement in L3 exceeds the calculated amount. For the parallel β-sheet, increasing the number of strands did not improve its agreement with the experiment. The finding of so few strands in sheets of membrane-assembled AcWL5 may be a consequence of experimental conditions. It is clear that much larger sheets are formed by AcWL5 in bilayers,[3] but we should expect supported monolayer membranes to be limited in the amount of peptide they can absorb because lateral pressure in the monolayer will increase when lipids are displaced by peptide. Differences in the number of β-strands per sheet is a plausible explanation for our finding that both the ^{12}C and ^{13}C bands in air-dried L3$-$lipid mixtures are observed at significantly lower frequencies than when L3 absorbs into monolayers (compare Figures 2 and 3).

Brauner et al. employed a transition dipole coupling approach in their study of a 14-residue peptide and achieved semiquantitative agreement between simulation and experiment by increasing the force constant between the interstrand hydrogen-bonded amide units.[23] We also found that by arbitrarily increasing the interstrand coupling energy (e.g., $V_{ns,(N-n+1)(s+1)} \approx -27$ cm^{-1}), the ^{13}C enhancement in the antiparallel case can roughly reproduce the experimental IR spectrum of the L2 peptide at a larger value of S. However, we have not found a physical basis for interstrand couplings of this magnitude. In

their ab initio calculations on the same 14-residue peptides, Kubelka et al. called attention to the contributions of in-phase interstrand coupling to the low-frequency amide-I$'$ mode.[24,25]

Conclusion

Our analysis of isotopically edited spectra supports our earlier conclusion that the β-structure formed by AcWL5 in phospholipid membranes is antiparallel and weighs strongly against the possibility that it is parallel. This supports the conventional interpretation of its widely split amide I band shape as representing antiparallel rather than parallel β-structure. Simulations incorporating through-bond and transition charge$-$transition charge interactions in an excitonic model can account for the enhancement of ^{13}C band intensities, and assuming there are three to four strands per antiparallel β-sheet, they yield acceptable agreement with experimental spectra. An important insight provided by these simulations is that both the interstrand nearest-neighbor coupling energy across the hydrogen bond and the sign of the intrastrand nearest neighbor coupling must be chosen correctly to permit adequate enhancement to occur. Therefore, couplings both along (through-bond) and across strand (through-space) are essential. The exciton band structure formed by the polypeptide amide units, the magnitude and sign of the vibrational anharmonic coupling energy, the zero-order energy shift of the ^{13}C isotope, and the number of strands are all important in determining the enhancement of the ^{13}C peak intensity. Other contributions, such as from the coupling between the peptide units ns and $ns + 2$ on the same strand, which have their amide-I$'$ motions in-phase, are less important. A comparable enhancement would not be expected for helical conformations, for which case the strongly allowed IR transition of the unperturbed system does not occur at the lowest level of the band and the zero-order isotope shift level exceeds the exciton bandwidth. Furthermore, less intensity transfer is expected in the case of ^{13}C$=$^{18}O substitution, which has a larger zero-order isotope shift of ca. 65 cm^{-1}.